Quantitative Image Analysis of HIV-1 Infection in Lymphoid Tissue

A. Haase
K. Henry
M. Zupancic
G. Sedgewick
R. Faust

SFI WORKING PAPER: 1996-07-045

SANTA FE INSTITUTE

Quantitative Image Analysis of HIV-1 Infection in Lymphoid Tissue

Ashley T. Haase*, Keith Henry, Mary Zupancic, Gerald Sedgewick, Russell A. Faust, Holly Melroe, Winston Cavert, Kristin Gebhard, Katherine Staskus, Zhi-Qiang Zhang, Peter J. Dailey, Henry H. Balfour, Jr., Alejo Erice, and Alan S. Perelson

A. T. Haase, M. Zupancic, W. Cavert, K. Gebhard, K. Staskus, Z.-Q. Zhang, Department of Microbiology, University of Minnesota Medical School, Minneapolis, MN 55455

K. Henry, H. Melroe, HIV Program, St. Paul-Ramsey Medical Center, St. Paul, MN 55101; Department of Medicine, University of Minnesota Medical School, Minneapolis, MN 55455

G. Sedgewick, Department of Cell Biology and Neuroanatomy, University of Minnesota Medical School, Minneapolis, MN 55455

R. A. Faust, Department of Otolaryngology, University of Minnesota Medical School, Minneapolis, MN 55455

H. H. Balfour, Jr., A. Erice, Department of Laboratory Medicine and Pathology, University of Minnesota Medical School, Minneapolis, MN 55455

P. J. Dailey, Chiron Corporation, Emeryville, CA 94608

A. S. Perelson, Theoretical Biology and Biophysics, Los Alamos National Laboratory, Los Alamos, NM 87545

* To whom correspondence should be addressed.

A quantitative technique was developed to determine HIV-1 viral burden in two important cellular compartments in lymphoid tissues (LT). Image analysis and in situ hybridization were combined to show that in the presymptomatic stages of infection there is a large pool of about 10^8 copies per gram of LT of viral RNA in virions on the surfaces of follicular dendritic cells, and a smaller pool of 10^3 to 10^5 (per gram) of infected cells with 20 to 200 copies of viral RNA. The concentration of viral RNA in these cells was found to be much less than in productively infected cells in culture, consistent with restriction of replication of HIV-1 in vivo by immune or other mechanisms. The agreement, however, between theoretical estimates of viral production in LT and clearance of virus from plasma suggest that sufficient virus could nonetheless be generated in LT to account for levels of virus detected in plasma, and that plasma assays may turn out to accurately mirror virus production in tissues. Tracking HIV-1 infection at the cellular level in tissue reservoirs provides opportunities to better understand the pathogenesis of infection and the impact of treatment.

Viral burden is a critical measure of the progress of HIV-1 infection and response to antiviral therapy that has been assessed largely by sampling the bloodstream, or, to a lesser extent, the lymphoid tissues (LT) that constitute a major reservoir and site of viral replication throughout much of the typically long course of HIV-1 infection (1–3). Because currently these assays determine the number of copies of viral RNA in a population of RNA molecules extracted from tissues or fluids, there is as yet little information about the magnitude of infection in cellular compartments that likely contribute to disease pathogenesis and respond to treatment in different ways. In LT, some viral RNA is contributed by mononuclear cells (MNCs), such as $CD4^+$ T lymphocytes, monocytes and macrophages, that produce virion progeny to perpetuate infection. Another significant fraction is in virions in immune complexes trapped by follicular dendritic cells (FDCs) in germinal centers within LT (1, 4). Although the sequestration of virus by FDCs may slow the spread of infection, the retention of infectious virions in immune complexes on FDCs (5) suggests that they could also be a continuing source of infection, even after effective antiviral therapy has largely suppressed virus production.

We developed and describe in this report an experimental approach to separately measure and evaluate viral burden in the MNC and FDC compartments in LT. To detect and distinguish HIV-1 RNA encapsidated in viral particles on the surfaces of FDCs from viral RNA in productively infected MNCs, we used in situ hybridization (6). HIV RNA in viral particles in immune complexes is distributed over the processes of FDCs and generates an easily recognizable diffuse hybridization signal in germinal centers (GCs) whereas the signal for MNCs is discretely localized to individual cells (1, 4). To quantitate viral RNA in these cellular compartments, we used radioactively labeled RNA probes (7) to generate hybridization signals consisting of silver grains overlying MNCs or associated with FDCs in radioautographs. We then calculated the number of copies of viral RNA from the number of silver grains, the specific activity of the

probes, length of radioautographic exposure, and efficiency of silver grain formation in tissue sections of 0.5 grains/dpm for ^{35}S (8). Assuming that the antisense probes hybridize with 100% efficiency and 1:1 stoichiometry, one copy of HIV-1 virion RNA should yield 2.4 grains for a radioautographic exposure of 24 hr.

We validated this calculation of copy number by applying it, under conditions comparable to those of our tissue assay, to a cell line in which the number of copies of HIV-1 RNA had been determined previously. By combining Northern blot analysis of extracted RNA with oligonucleotide probes specific for unspliced, singly spliced, and multiply spliced viral RNAs, ACH-2 cells had been shown (9) to contain 300 to 400 copies of virion RNA. We injected ACH-2 cells into a mouse spleen and fixed and processed paraffin-embedded tissues as described for the tissues (6). We enumerated silver grains over 100 ACH-2 cells in tissue sections of the spleen and calculated, as described above, a mean number of 350 genome equivalents per cell, in excellent agreement with the previously published determinations (9).

We assessed the sensitivity and specificity of the assay in this system and in LT by comparing the signal generated by in situ hybridization with antisense and sense HIV-1 RNA probes. For the radioautographic exposure time of one day that we used to maintain the clear discrimination between the signal from FDCs and MNCs, the background over MNCs and GCs with the sense probe was negligible; and the limits of detection with the antisense probe was 20 copies of viral RNA per cell.

To routinely enumerate silver grains in sections of LT, we combined in situ hybridization and quantitative image analysis (10). There were so many positive GCs in LT, and so many silver grains in each GC, that it was impractical to enumerate grains at high magnification. We therefore obtained video images of positive GCs at relatively low magnification and deconstructed and analyzed the image at higher magnification where the number of silver grains could be accurately scored. The deconstruction and reconstruction of an image of a positive GC is illustrated in Fig.

1A, B. We were unable to reproducibly enumerate grains by analysis of bright-field images but we could determine grain counts in video images of LT section illuminated with epipolarized light. In this case, because nearly all of the light is reflected from the grains, the gray values of the images of silver grains are much less than the background and can be distinguished by setting a threshold. Only those images of silver grains with gray levels less than the threshold set for each video image and highlighted by a red overlay in Fig. 1C were measured (Fig. 1D. From an empirically determined relationship of the standard area of a single silver grain at this magnification we obtained values for the total number of silver grains in the image. We periodically repeated this procedure to confirm the relationship of standard area to the number of silver grains. In this 8-μM section of a positive GC, about 13,000 grains were measured, equivalent to 5,400 genome equivalents of viral RNA and 2,700 virions.

HIV gene expression in $CD4^+$ T lymphocytes, monocytes and macrophages has been previously shown to be distributed across a spectrum ranging from a few copies per cell, detectable only after amplification in situ or long radioautographic exposures, to cells whose viral RNA content can be two orders of magnitude higher (1, 11). It is the latter cells that presumably are the primary producers of new virus; the cells that contribute to immune depletion by elimination by host defenses or as a consequence of the cytopathic effects of viral replication; and the cells that should decrease in frequency in response to antiretroviral therapies that block new infections.

The transcriptionally most active MNCs with 20–200 genome equivalents of HIV-1 RNA are easily and unambiguously identified in radioautographs of sections of LT after in situ hybridization (Fig. 2A). Because only the silver grains stand out in the image of the section illuminated with epipolarized light alone (Fig. 2B), setting the threshold to discriminate the grains from background (Fig. 2C) and measuring the thresholded area, as described for the GC, is straightforward. Again, by empirically determining, in this case at 400X, the relationship between

area of the objects above the threshold and a standard area for a single grain, we obtained the number of grains per MNC. The estimates of copy number were quite reproducible, varying <10% in ten independent measurements of individual MNCs (not shown).

To estimate total body viral burden in each cellular compartment in LT, we determined the number of copies of viral RNA on a per gram basis. We first measured the areas of LT in the tissue sections. More than 90 percent of the area in the tonsillar biopsy tissue was comprised of LT (Fig. 3A) whereas in tissue sections of spleen the LT (white pulp) made up only 10–20 percent of the sample. From the measurements of area, nominal thickness (8 μm), and density (about 1 gm/cm^3 of LT) the data from image analysis could be expressed as copies of viral RNA per gram of LT.

We used quantitative image analysis and in situ hybridization to assess HIV burden in cellular compartments in LT in cross-sectional and longitudinal studies of nine HIV-1-infected individuals. These individuals were largely asymptomatic and, with one exception, were receiving antiretroviral treatment (Table 1A). We focused in seven of the nine cases on LT obtained by biopsy of tonsillar tissue, because tonsil is an accessible source of LT that can be biopsied frequently and repeatedly in an outpatient clinic setting (12). For comparison of tonsil with other LT, we analyzed spleen and lymph node tissue from one individual, and spleen from another.

What is immediately striking in the calculated pool sizes summarized in Table 1A is the predominance of the FDC component. The amount of HIV-1 RNA associated with FDCs exceeded on average by 40-fold the amount of viral RNA in the MNC population that had the highest levels of viral RNA in vivo. Because most of the HIV-1 RNA was in the FDC compartment, this pool should contribute most of the RNA measured after extraction from LT and there should be reasonable agreement between the number of copies of viral RNA in the FDC pool and the total viral RNA burden in extracted RNA. We tested this prediction by comparing the cellular and population measurements of viral burden in two individuals from whom we obtained simultaneous samples of right and left tonsil to control for sample variation. Within the

approximate two- to three-fold variation between samples, there was in fact the predicted agreement of viral RNA estimated by branched DNA assay and by in situ hybridization and quantitative image analysis (Table 1B).

In the four individuals from whom sequential tonsillar biopsies were obtained over the course of more than a year (patients 4 to 7 in Table 1A), the concentration of HIV RNA associated with FDCs ranged from about 10^7 to $>10^8$ copies per gram. Tonsillar tissue appears to be representative of LT, as pool sizes of HIV-1 RNA were comparable in single tonsillar specimens, lymph nodes and spleen from the same or different individuals (see patients 8 and 9 in Table 1A). Taking the mean of about 10^8 copies of HIV-1 RNA per gram as representative of steady state HIV-1 burden in the FDC pool (Table 1A), and 1% as the fraction of body weight in LT (13), the FDC-associated pool of HIV RNA would be about 10^{11} copies in a 70-kg HIV-infected individual. The relative magnitude of this reservoir can be appreciated by comparing the concentrations of HIV-1 RNA in the FDC pool with plasma (Table 1A). The FDC pool is greater than plasma RNA by factors of 10^2 to $>10^4$ and, at times when viral RNA was below the detection level of the assay (5×10^3), there were $>10^8$ copies of viral RNA per gram LT associated with FDCs.

The size of the FDC-associated pool of viral RNA was not related to clinical stage, CD4 count or treatment. In the four individuals studied longitudinally, the size of the pool was relatively stable, and infrequently exceeded 5×10^8 copies per gram. These initial findings are consistent with a large but saturable pool of trapped HIV and with the proposed roles of the FDCs both as a potential source of infectious virions (5), and local mechanism to sequester and slow the systemic spread of HIV-1 (14).

The number of copies of HIV-1 RNA in approximately 1,200 MNCs in LT in the nine individuals we studied was lower than the intracellular concentration of viral RNA in ACH-2 cells (9) or in cultures of phytohemagglutinin-stimulation peripheral blood MNCs (PBMC) from an

uninfected individual. Five days after infecting the PBMC culture with HIV-1 at a multiplicity of 0.1 $TCID_{50}$ per cell, we measured an average of 1,100 copies per cell, range of 150–3,800 copies per cell (not shown) compared to 74 copies and a range of 20–286 copies per cell in vivo (Table 1A). We show in Figure 4 representative frequency distributions of viral RNA in MNCs in vivo, and in culture, to illustrate the low frequency of cells in vivo with >200 copies of viral RNA and the overall reduction in viral RNA in these cells vis-a-vis ex vivo infections.

We interpret the reduced levels of viral RNA in vivo as evidence of constraints on replication imposed by the immune system or other mechanisms. The distribution of intracellular RNA content in vivo we assume reflects the different stages of the viral life cycle in individual cells in which replication was initiated asynchronously. Cells with fewer copies of viral RNA would represent cells in the earlier stages of the viral life cycle and those with higher concentrations of intracellular viral RNA would be cells at more advanced stages of viral replication. The increasing likelihood of recognition and elimination by cytotoxic T lymphocytes of infected cells at the later productive phase of the life cycle could account for the lower mean number of copies of viral RNA and frequency of cells with >200 copies per cell in vivo. Alternatively, suppression of virus gene expression by $CD8^+$ T lymphocytes and cytokines (15) or other factors could be responsible for the restricted replication of HIV-1 in vivo.

The frequency of productively infected MNCs varied considerably between individuals, and within individuals over time. There was again no obvious relationship to clinical status, CD4 count, or treatment. What the turnover of this population contributes to immune depletion cannot be derived from in situ "snapshots" alone but we can advance some conjectures based on studies of viral dynamics in the bloodstream (16, 17) where the turnover of productively infected cells has been modeled by the term δT^*, in which $\delta \sim 0.5$ day^{-1} is the death rate of productively infected cells, and T^* is the number of productively infected cells (17). Using this formula, the mean daily turnover rate for productively infected cells would be $0.5T^* = 0.5 \times 5.3 \times 10^4$ per gram (Table

1A) or 2 X 10^7 cells per day for a 70-kg individual. This calculated turnover rate is substantially lower than the $CD4^+$ T lymphocyte turnover of $>10^9$ cells per day estimated from dynamic studies (16), and may indicate that the loss of $CD4^+$ T cells is linked to infection but is not only the result of elimination of productively infected cells. This conclusion, however, must be qualified as there are likely many more infected cells with <20 genome equivalents of HIV-1 RNA (1, 11) not measured in our assay that nonetheless might have sufficient levels of viral gene expression to be recognized and destroyed by immune surveillance mechanisms. Assays of greater sensitivity will be needed to evaluate the contribution of MNCs with these lower levels of viral gene expression to immune depletion.

Estimates of viral production have thus far been derived from measurements of plasma HIV-1 RNA over time (17) which suggest that there is a quasi-steady state in which viral production is balanced by viral clearance. Perelson *et al.* (17) model the rate of virus production by the term $N\delta T^*$, where N is the total number of virions produced by a productively infected cell during its lifetime, and the rate at which virus is cleared is modeled by the term cV, where the viral clearance rate constant $c = 3$ day^{-1}, and V is the viral load. The estimates of c and δ were derived from examination of HIV-1 in plasma only, and are minimal estimates (17). Since most of the infected cells producing virus are in LT, we used the data in Table 1A to examine the relationship between viral production in tissues and clearance in more detail. The relationship of intracellular viral RNA concentration to the number of virions produced by the cell is unknown but with the rationale that most of viral RNA is destined to be encapsidated in virions in the late stages of infection, we approximated N as one-half of the maximum of the number of copies of HIV RNA per MNC (Table 1A). With these assumptions we find that cV is on average equal to $N\delta T^*$ (Table 1A). Given the current uncertainties in estimating c, N and T^*, the agreement is remarkable and suggests that plasma levels of HIV may reflect LT production of virus within the limits of the assays.

Quantitative analysis of infection at the cellular level in tissues is a technology that affords opportunities to better understand the pathogenesis of HIV-1 infection and a way to directly monitor the impact of antiviral treatment in the principal tissue reservoir. We can now apply this approach to ask whether there is a state of virologic regression with potent antiretroviral therapy analogous to cancer chemotherapy. A successful response would be indicated by reduction in the number of productively infected cells, and, perhaps, slower decay of viral burden in the FDC compartment that parallels a fall in HIV RNA levels in plasma to undetectable levels. With image analysis it will be possible to determine the kinetics and extent of clearance of HIV from these LT reservoirs. The preliminary indications in this report that production of HIV in LT is reflected in plasma viral burden provides a basis to be optimistic that there will be evidence of remission or cure in LT congruent with results in the most accessible compartment, the bloodstream. If this turns out to be the case, then the blood compartment can be monitored with the confidence that it accurately reflects the long-term effectiveness of current and emerging therapies. If not, LT viral burden will need to be monitored in at least a subset of subjects to evaluate the benefit of candidate retroviral therapies.

References and Notes

1. J. Embretson *et al., Nature* **362,** 359 (1993).

2. G. Pantaleo *et al., Nature* ibid., p. 355 (1993).

3. G. Pantaleo *et al., Proc. Natl. Acad. Sci. U.S.A.* **88,** 9838 (1991).

4. C. H. Fox *et al., J. Infect. Dis.* **164,** 1051 (1991); K. Tenner-Rácz *et al., AIDS* **2,** 299 (1988); H. Spiegel, H. Herbst, G. Niedobitek, H.-D. Foss, H. Stein, *Am. J. Pathol.* **140,** 15 (1992); J. Schmitz *et al., J. Immunol.* **153,** 1352 (1994).

5. S. L. Heath, J. G. Tew, J. G. Tew, A. K. Szakal, G. F. Burton, *Nature* **377,** 740 (1995).

6. L. M. Angerer, M. H. Stoler, R. C. Angerer, in *In Situ Hybridization. Applications to Neurobiology*, K. L. Valentino, J. H. Eberwine, J. D. Barchas, Eds. (Oxford University Press, New York, NY, 1987), pp. 42–70.; A. T. Haase, in *In Situ Hybridization. Applications to Neurobiology*, K. L. Valentino, J. H. Eberwine, J. D. Barchas, Eds. (Oxford University Press, New York, NY, 1987), pp. 197–219. In preliminary experiments, conditions for obtaining, fixing and processing tissue specimens were optimized. To eliminate autolysis as a variable, tissue samples were fixed within minutes of biopsy. Optimal conditions for fixation were determined in preliminary experiments to be immersion in 4% paraformaldehyde for 4 to 6 hours followed by transfer to 70 to 80% ethanol and paraffin embedding; or at least 24 hours to 7 days in Streck's tissue fixative and subsequent processing as described for paraformaldehyde. These conditions were established by comparisons of signal generated by in situ hybridization in portions of tonsillar biopsies fixed in different ways for varying times. For in situ hybridization, sections of 8 μm of paraffin-embedded fixed tonsillar biopsies and other lymphoid tissues were cut, adhered to silanized glass slides, and deparaffinized through xylene and graded alcohols. Prior to hybridization the sections were treated as described in the reference cited above. In brief, slides were immersed in 0.2 N HCl for 30 min., 0.15 M triethanolamine pH 7.4 for 15 min., and 0.005% digitonin for 5 min., all at room temperature.

The slides were then incubated for 15 min. at 37°C in a buffered solution containing 2 mM $CaCl_2$ and proteinase K (5 µg/ml). We found that these pretreatments resulted in equivalent or higher signal over GCs than higher concentrations of proteinase K that had been described (6). After removing and washing the slides, they were acetylated (0.25% acetic anhydride) for 10 min., and then dehydrated through graded solutions of ethanol. The sections were then covered with hybridization solution [50% deionized formamide, 10% dextran SO_4, 0.6 M NaCl, yeast tRNA (0.4 mg/ml), 1X Denhardt's medium, in 20 mM Hepes buffer pH 7.2 with 1 mM EDTA and 40 mM dithiothreotol (DTT)] containing 10^5 cpm/µl of ^{35}S RNA probe. The solution was sealed under a coverslip with rubber cement and the slides were incubated 24 hours at 45°C. After removing the coverslips, the slides were immersed in 5 X SSC, and washed as follows: 5 X SSC, 10 mM DTT, 42°C, 30 minutes; 2 x SSC, 50% formamide, 10 mM DTT, 60°C, 20 minutes; 2 X RWS (0.1 M tris-HCl, pH 7.5, 0.4 M NaCl, 50 mM EDTA), 10 min. The sections were then digested at 37°C with ribonucleases A, 25 µg/ml, and T1, 25 µ/ml, in RWS for 30 min.; washed at 37°C in RWS for 15 min.; 2 X SSC, 37°C for 15 min.; 0.1 x SSC, 37°C for 15 min.; dehydrated through graded alcohols containing 0.3 M ammonium acetate, dried, and coated with Kodak NTB-2 emulsion. After radioautographic exposures of 24 hours at 4°C, the slides were developed and stained for one minute in Wright's stain.

7. For in situ hybridization, riboprobes complementary to about 90 percent of the sequences in full-length HIV genomic RNA were purchased from Lofstrand Labs Limited (Gaithersburg, MD) as sense or antisense transcripts of the cloned restriction fragments. The RNA probes were labeled by incorporation of ^{35}S-CTP to specific activities of 6 to 8 X 10^8 dpm/µg.

8. A. W. Rogers, *Techniques of Autoradiography*, 3rd ed., (Elsevier/North Holland Biomedical Press, Amsterdam, 1979), pp. 102–103.

9. H. Peng *et al.*, *Virology* **206,** 16 (1995).

10. For image analysis, radioautographs were illuminated with epipolarized light, using an Olympus mercury light source and the differential interference cube of the Olympus B-max microscope. Video images were captured with a low-light cooled CCD camera (Optronics TEC-470) and Image 1/MetaMorph Version 2 software (Universal Imaging Corporation, Westchester, PA 19380, U.S.A.). Silver grains were differentiated from background and measured with the "threshold" and "measure object" tools of the MetaMorph software. The relevant GCs and MNCs in the image were delineated with the tracing tool. On the basis of analyses illustrated in Fig. 1, measurement parameters for standard area of a single grain in the MetaMorph system were set at each magnification to obtain grain counts. Data was recorded on a Microsoft Excel spreadsheet.

11. B. K. Patterson *et al., Science* **260,** 976 (1993); G. J. Nuovo, F. Gallery, P. MacConnell, A. Braun, *Am. J. Pathol.* **144,** 659 (1994); G. J. Nuovo, A. Forde, P. MacConnell, R. Fahrenwald, ibid., 40 (1993).

12. R. A. Faust *et al., Otolaryngol. Head Neck Surg.* **114,** 593 (1996).

13. P. Lydyard and C. Grossi, in *Immunology,* I. Roitt, J. Brostoff, D. Male, Eds., (J. B. Lippincott, Philadelphia, PA, 1989), pp. 2.1–2.18.

14. G. Pantaleo and A. S. Fauci, *Ann. Rev. Immunol.* **13,** 487 (1995); B. F. Haynes, G. Pantaleo, A. S. Fauci, *Science* **271,** 324 (1996).

15. C. M. Walker, D. J. Moody, D. P. Stites, J. A. Levy, *Science* **234,** 1563 (1986); J. E. Brinchmann, G. Gaudernack, F. Vartdal, *J. Immunol.* **144,** 2961 (1990); C. M. Walker, A. L. Erickson, F. C. Hsueh, J. A. Levy, *J. Virol.* **65,** 5921 (1991); M. Baier, A. Werner, N. Bannert, K. Metzner, R. Kurth, *Nature* **378,** 563 (1995); F. Cocchi *et al., Science* **270,** 1811 (1995); S. M. Wolinsky *et al., Science* **272,** 537 (1996).

16. J. M. Coffin, *Science* **267,** 483 (1995); X. Wei *et al., Nature* **373,** 117 (1995); D. Ho *et al.,* ibid., 123 (1995).

17. A. S. Perelson, A. U. Neumann, M. Markowitz, J. M. Leonard, D. D. Ho, *Science* **271,** 1582 (1996).

18. C. Pachl *et al., J. Acquir. Immune Defic. Syndr.* **8,** 446 (1995); R. L. Dewar *et al., J. Infect. Dis.* **170,** 1172 (1994); Y. Cao *et al., AIDS Research & Human Retroviruses* **11,** 353 (1995).

19. We thank S. Wietgrefe and the reviewers for helpful comments, C. O'Neill and T. Leonard for preparation of the manuscript and figures, the Ramsey Foundation, the Santa Fe Institute, and the Joseph P. and Jeanne M. Sullivan Foundation,and the National Institutes of Health (grants AI 28246, AI 27661 and RR 06555) for support. Portions of this work were done under the auspices of the United States Department of Energy.

TABLE 1A. ***In Situ*** **Hybridization and Quantitative Image Analysis of HIV-1 RNA Levels in LT**

Patient no.	Age	CDC class	Treatment	CD4 count/ mm^3 blood	Sample	Number of HIV RNA equivalents per ml of plasma (bDNA assay)	Number of copies of HIV RNA /gm tissue		Average no. and range ( ) of copies of HIV RNA / MNC	Frequency of productively infected MNCs/gm tissue	$\frac{cV}{N\delta T^*}$
							FDCs	MNCs			
1	26	B3	ZDV/3TC	114	tonsil, right	4×10^4	2.3×10^8	2.4×10^6	62 (20–188)	3.8×10^4	0.7
					tonsil, left		4.9×10^8	3.9×10^6	86 (30–259)	4.5×10^4	
2	32	A2	ZDV/DLV	375	tonsil, right	$<5 \times 10^3$	1.6×10^8	2.9×10^6	73 (26–130)	4×10^4	
					tonsil, left		9.2×10^7	1.9×10^6	58 (36–118)	3.3×10^4	
3	31	A1	ZDV	638	tonsil	$<5 \times 10^3$	3.2×10^8	8.6×10^5	62 (23–140)	1.4×10^4	
4	45	A1	none	551	tonsil, baseline	10^4	1.9×10^8	1.6×10^6	76 (28–214)	2×10^4	0.3
					tonsil, + 1 mo.		1.6×10^8	1.3×10^5	79 (24–234)	1.6×10^3	
				763	tonsil, + 6 mo.	$<5 \times 10^3$	5.4×10^8	4.6×10^5	150 (20–287)	3×10^3	
					tonsil, + 12 mo.		4.3×10^8	1.4×10^7	79 (21–188)	1.8×10^5	
				437	tonsil, + 14 mo.	1.4×10^4	3.4×10^8	4×10^6	94 (20–180)	4.2×10^4	0.2
5	32	A2	ZDV	294	tonsil, baseline	$<5 \times 10^3$	10^8	8×10^4	80 (20–97)	10^3	
					tonsil, + 1 mo.		6.2×10^7	8×10^4	80 (20–108)	10^3	
			ZDV/DLV	215	tonsil, + 6 mo.	$<5 \times 10^3$	6.3×10^7	7.5×10^4	75 (49–91)	10^3	
			none	202	tonsil, +12 mo.	$<5 \times 10^3$	7×10^7	3×10^6	58 (20–151)	5.1×10^4	
				197	tonsil, + 14 mo.	$<5 \times 10^3$	5×10^7	3.4×10^6	57 (20–106)	6×10^4	
6	32	A1	none	633	tonsil, baseline	7.6×10^4	2.3×10^7	3.9×10^6	38 (20–141)	10^5	0.7
					tonsil, + 1 mo.		1.3×10^7	2.2×10^6	72 (20–177)	3×10^4	
			ZDV/ DDC	389	tonsil, + 12 mo.	$<5 \times 10^3$	5.8×10^7	1.7×10^6	41 (20–115)	4×10^4	

Patient no.	Age	CDC class	Treatment	CD4 count/ mm^3 blood	Sample	Number of HIV RNA equivalents per ml of plasma (bDNA assay)	Number of copies of HIV RNA /gm tissue		Average no. and range ( ) of copies of HIV RNA / MNC	Frequency of productively infected MNCs/gm tissue	$\frac{cV}{N\delta T^*}$
							FDCs	MNCs			
7	48	A1	ZDV	782	tonsil, baseline	2.6×10^4	4.2×10^6	1.8×10^6	124 (48–222)	1.5×10^4	1
					tonsil, + 1 mo.		7.6×10^7	1.9×10^7	74 (20–183)	2.6×10^5	
				778	tonsil, + 6 mo.	2.9×10^4	1.8×10^8	6×10^5	85 (50–188)	7.1×10^3	2.8
				615	tonsil, + 14 mo.	7.6×10^4	3.2×10^7	10^7	44 (20–136)	2.3×10^5	0.3
8	37	A3	D4T	140	spleen	$<5 \times 10^3$	7.9×10^6	1.8×10^5	58 (45–77)	3.1×10^3	
9	39	A2	DDC	245	lymph node	$<5 \times 10^3$	3.8×10^7	1.1×10^6	63 (28–124)	1.7×10^4	
			none	106	spleen	2×10^5	7×10^7	5.7×10^6	63 (20–128)	9×10^4	2.2
Mean:				402			1.5×10^8	3.4×10^6	74	5.3×10^4	1.0

3TC = Lamivudine/Epivir; D4T = Stavudine/Zerit; DDC = Zalcitabine/HIVID; DLV = Delavirdine; ZDV = Zidovudine/Retrovir.

LT were obtained from HIV-1-infected individuals in the CDC clinical stage shown and with the CD4 counts indicated. Tissues were fixed by immersion for 4–5 hours in 4 percent paraformaldehyde or for at least 24 hours in Streck's tissue fixative. The number of copies of HIV-1 RNA was determined by in situ hybridization and quantitative image analysis. HIV-1 RNA levels per ml of plasma were determined by bDNA assay in samples taken at the time of tonsil biopsy. The viral clearance rate, cV, was calculated assuming $c = 3$ day^{-1} (17) and that V is the total viral load in extracellular fluid calculated by dividing the number of HIV RNA equivalents per ml of plasma by 2, and then multiplying the 15×10^3 ml of extracellular fluid in a 70-kg individual. With the rationale described in the text, N was taken to be the maximum of the range of the number of copies of HIV RNA/MNC divided by 2. T^* was taken to be the frequency of productively infected MNCs/gm tissue multiplied by the assumed 700 gm of LT per 70-kg individual, and $\delta = 0.5$ day^{-1} (17). Both N and T^* will be underestimates, as on average only about 75 percent of a productively infected MNC will be analyzed in a section 8 μm in thickness; and because T^* will not include infected cells with fewer than 20 copies of viral RNA.

TABLE 1B. Comparison of Single-Cell and Population Estimates of HIV-1 RNA

Patient no.	Age	CDC class	Treatment	CD4 count/ mm^3 blood	Sample	Number of copies of HIV RNA associated with FDCs per gm of tonsillar tissue	
						In situ hybridization	bDNA assay
1	26	B3	ZDV/3TC	110	right tonsil	2.3×10^8	3.9×10^8
					left tonsil	4.9×10^8	5.2×10^8
2	32	A2	ZDV/DLV		right tonsil	1.6×10^8	8.1×10^7
				375	left tonsil	9.2×10^7	8.5×10^7

Simultaneous biopsies of right and left palatine tonsil were obtained and divided into two weighed fragments. One portion was snap frozen, and at a later time RNA was extracted and the number of HIV RNA equivalents determined by branched DNA (bDNA) assay (18). The other portion was fixed, sectioned at a later time and viral RNA associated with FDCs quantitated as described in this report.

Figure Legends

Fig. 1. Quantitative image analysis of HIV RNA associated with FDCs in GCs. (**A** and **B**). A video image at low magnification (160X) of the diffuse hybridization signal of FDC-associated HIV RNA in a GC in a section of tonsil was deconstructed and analyzed at higher magnification (600X). The area highlighted in green in **A** is shown in **B** at the higher magnification, where silver grains could be accurately enumerated. The scored images were then reconstructed as indicated by the areas highlighted by white lines. (**C**). Objects in the image above a set threshold are shown in red. In sections illuminated with epipolarized light, these are nearly exclusively silver grains that reflect the light. This thresholded image was then measured, as shown in **D**. Colors in **D** identify measured objects.

Fig. 2. Quantitative image analysis of HIV RNA in MNCs with the most abundant viral transcripts. **A.** A MNC with HIV RNA in a radioautograph of a section of tonsil, bright-field and epipolarized illumination 400X. The specular reflectance from the silver grains overlying the MNC with HIV RNA imparts a green-white hue to the grains in the color video image. **B.** Image shown in A, epipolarized illumination. **C.** Image of **B** after threshold evaluation, as described in Fig. 1. **D.** The measured area of the MNC in C.

Fig. 3. Determination of LT area by image analysis. **A.** The MetaMorph tracing tool was used to trace (in red) a submucosal region of LT in a section of a tonsillar biopsy (20X). The area in pixels was converted to mm^2 by applying a calibration relating to pixel area to mm^2 from a 20X image of a 2 mm scale with 0.1 mm divisions. **B.** LT area in the white pulp in a section of spleen. The more darkly stained white pulp has been segregated (colored traces) and all individual areas added together.

Fig. 4. A comparison of intracellular concentrations of HIV RNA in vivo and in productively infected cultures. The number of copies of HIV RNA was measured in MNCs in LT and MNCs from peripheral blood monocytes (PBMC) infected with HIV-1. Shown are representative

frequency distributions of tonsillar biopsies from four patients and the culture. Time 1 and time 2 refer to biopsies obtained at different times in patient 1; R and L refer to right and left tonsillar biopsies obtained at one time from patient 4.

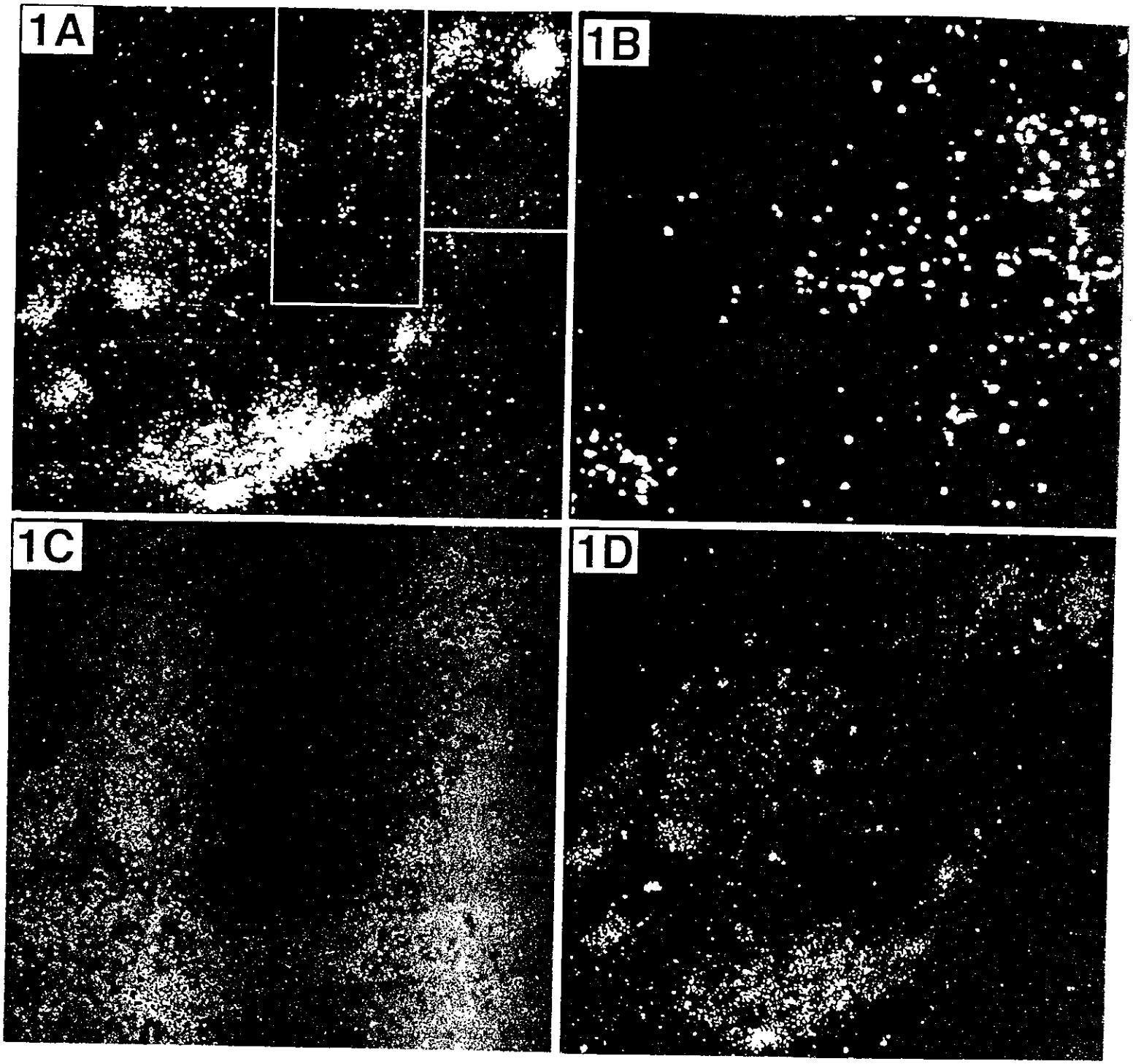
1A
1B
1C
1D

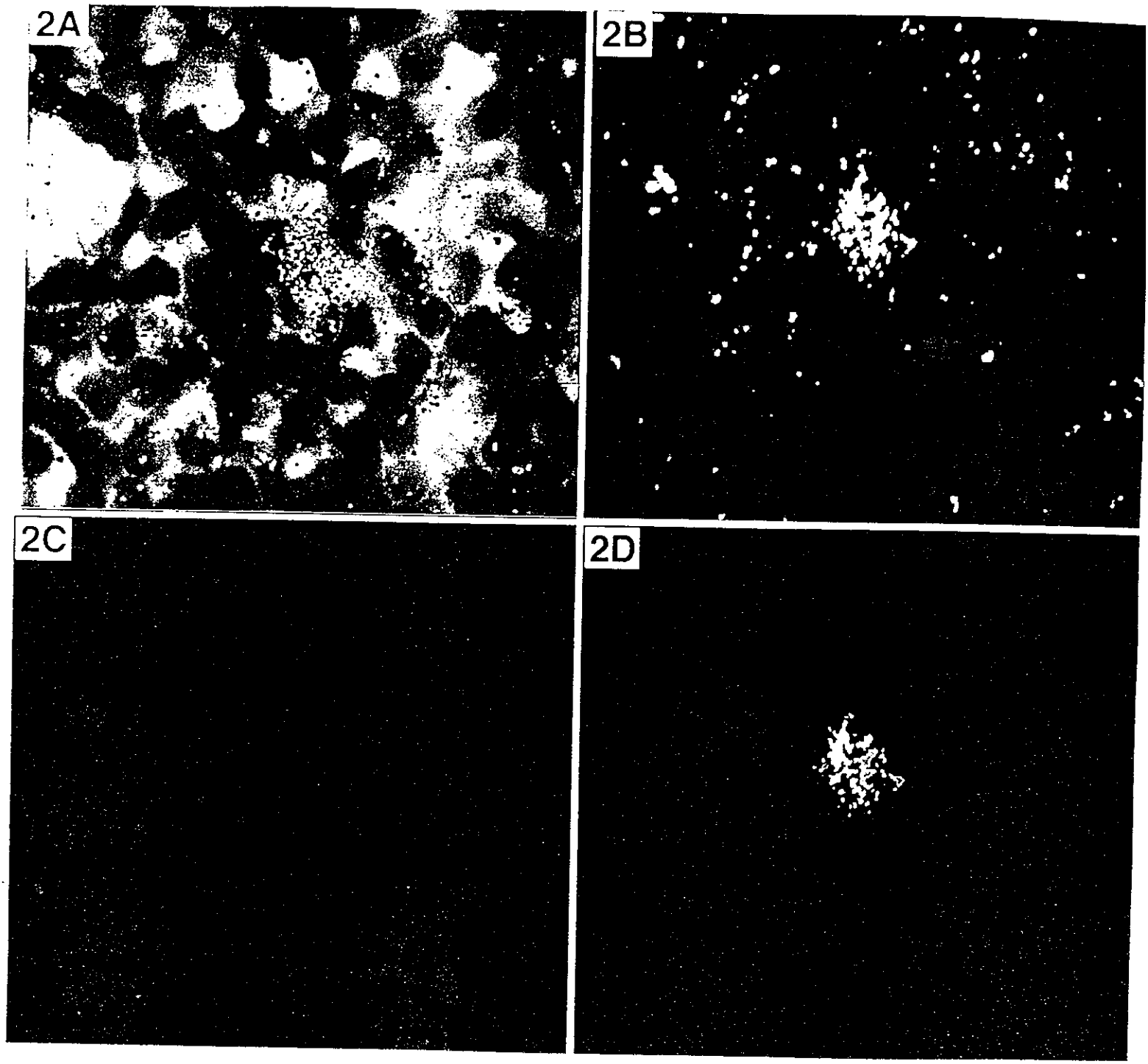
2A
2B
2C
2D

3A

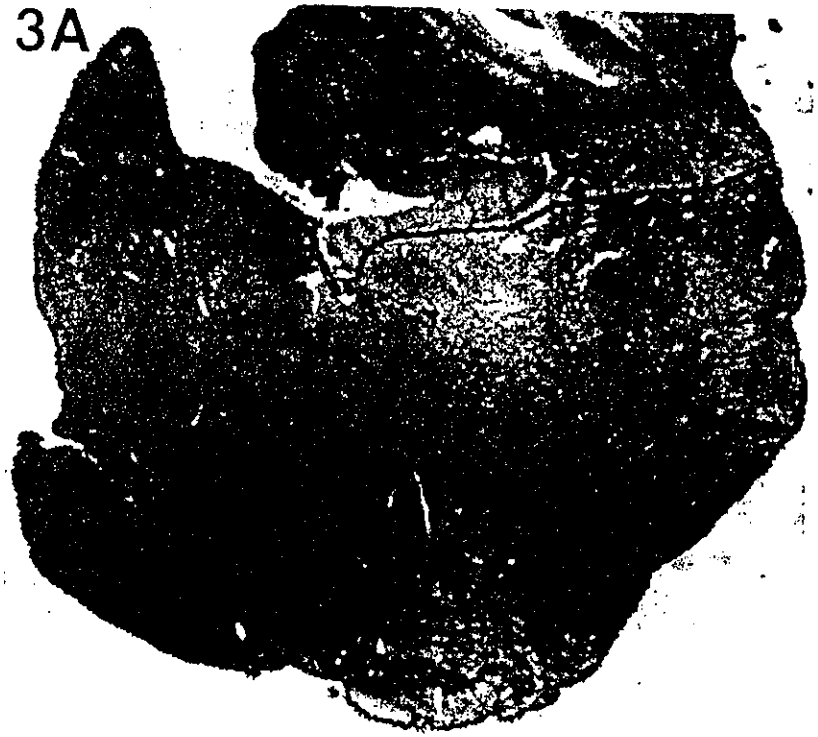

3B

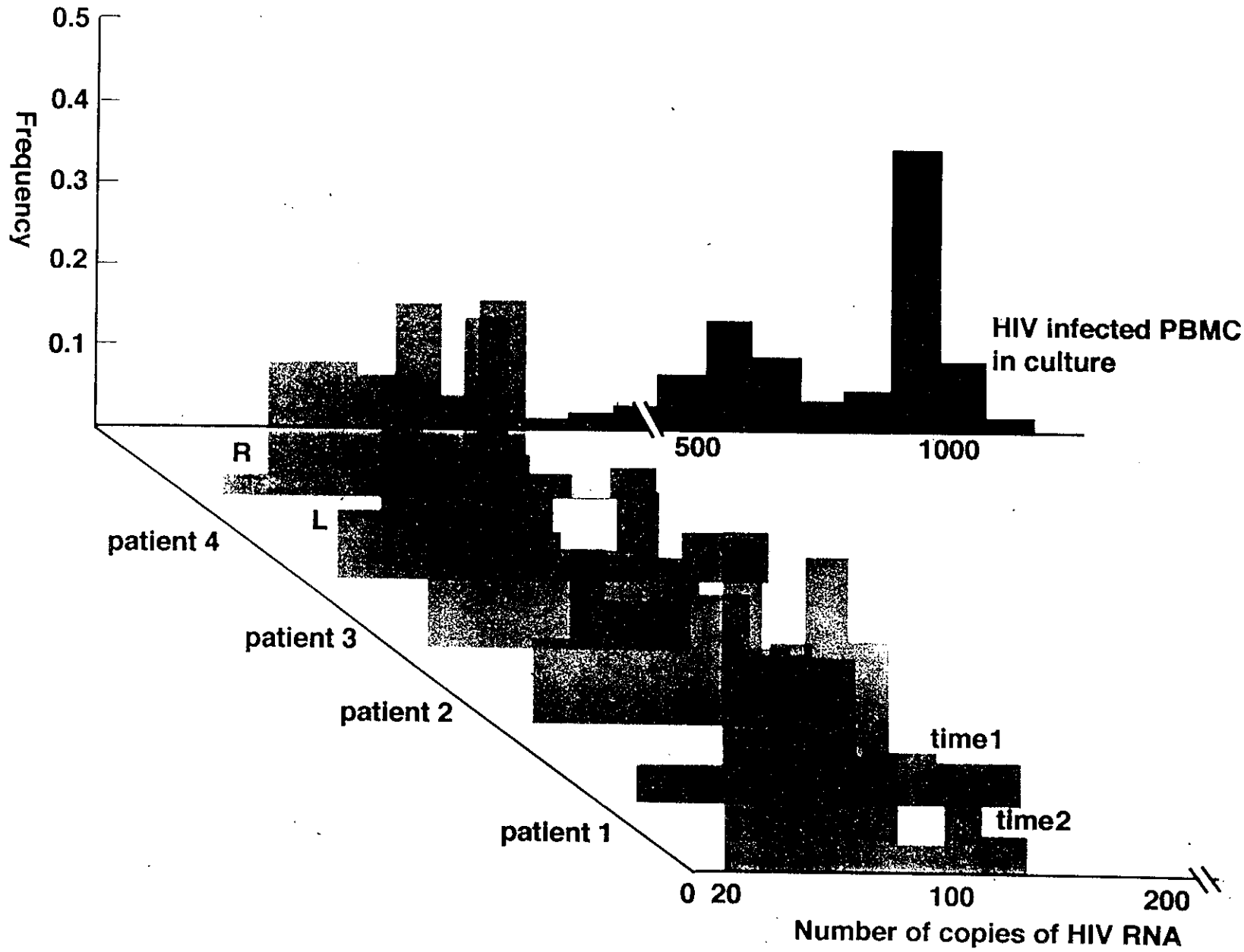
0.5
0.4
0.3
0.2
0.1
Frequency
HIV infected PBMC
in culture
R
L
500
1000
patient 4
patient 3
patient 2
patient 1
time1
time2
0
20
100
200
Number of copies of HIV RNA